Cancer Management and Research

Elevate Series

Open Access Full Text Article

ORIGINAL RESEARCH

Comparative Diagnostic Performance of Digital Versus Analog PET/CT for Lymph Node Metastases and Glut-1 Correlation in Resected Non-Small Cell Lung Cancer

Katsuhiko Shimizu[1], Yoshihiko Fukukura[2], Shinsuke Saisho[1], Yuji Nojima[1], Shogo Takeuchi[2], Takashi Matsutani[1], Hiroki Sugiyama[1], Masao Nakata[1]

[1]Department of General Thoracic Surgery, Kawasaki Medical School, Kurashiki, Okayama, Japan; [2]Department of Radiology, Division of Functional and Metabolic Imaging, Kawasaki Medical School, Kurashiki, Okayama, Japan

Correspondence: Katsuhiko Shimizu, Department of General Thoracic Surgery, Kawasaki Medical School, Matsushima 577, Kurashiki, Okayama, 701-0192, Japan, Tel/Fax +81-86-464-1124, Email kshimizu@med.kawasaki-m.ac.jp

Cancer Management and Research downloaded from https://www.dovepress.com/
For personal use only.

Background: Recent innovations in technology have significantly advanced the imaging capabilities of positron emission tomography/computed tomography (PET/CT). Digital PET/CT provides sensitive and high-resolution imaging and can improve the detection of small lesions as compared to conventional (analog) PET/CT. This study aimed to compare the diagnostic performance of digital versus analog PET/CT for detecting lymph node metastases and to assess the maximum standardized uptake (SUVmax) values in patients with resected non-small cell lung cancer (NSCLC).

Methods: We enrolled a total of 103 patients with lung adenocarcinoma or squamous cell carcinoma who had undergone preoperative PET/CT in either analog or digital scanners. The primary endpoint was comparison of the diagnostic performance of the two modalities for lymph node metastasis, and the secondary endpoints were comparison of the SUVmax values and correlation of the SUVmax values with the Glut-1 (glucose transporter type 1) expression.

Results: Of the 103 patients enrolled in the study, 61 had undergone analog PET/CT, and 42 had undergone digital PET/CT. Significantly higher SUVmax values on digital as compare with analog PET/CT were obtained for cT1b tumors (D/A ratio = 3.42, $p = 0.002$) as well as cT1c tumors (D/A ratio = 2.10, $p < 0.001$). However, no significant difference in SUVmax values between the two types of PET/CT was obtained for tumors exceeding 3.0 cm in diameter. A stronger correlation was found between tumor Glut-1 expression and the SUVmax values obtained digital PET/CT as compared with the values obtained with analog PET/CT. Digital PET/CT also showed a higher sensitivity (71.4% vs 37.5%) for detecting lymph node metastases, although the specificity was slightly lower (88.6% vs 96.2%), and the overall accuracy was comparable (85.7% vs 88.5%) between the two types of scanners. False-positive lymph nodes on digital PET/CT were obtained in conditions such as pneumoconiosis and anthracosis, while false-negatives results were obtained in conditions such as micrometastases and/or low lymph node Glut-1 expression.

Conclusion: These results suggest that digital PET/CT shows improved diagnostic sensitivity and that the results of digital PET/CT are better correlated with tumor metabolic activity, which results in improved detection of lymph node metastases. These results support the clinical usefulness of digital PET/CT for optimizing perioperative strategies and increasing diagnostic confidence in the management of NSCLC. Future multicenter prospective studies and a standardized redefinition of SUVmax are urgently needed to validate our findings and to establish more reliable clinical application of digital PET/CT in patients with lung cancer.

Keywords: digital PET/CT, SUVmax, lymph node metastases, Glut-1

Introduction

Fluorine-18 fluorodeoxyglucose positron emission tomography/computed tomography (FDG-PET/CT) has become an important tool for the diagnosis and staging of non-small cell lung cancer (NSCLC).[1] The maximal standardized uptake values (SUVmax) of primary tumors have been shown to be correlated with the disease stage, nodal status, histological type, differentiation grade, and progression of the tumors in patients with NSCLC.[2–4]

Received: 26 May 2025
Accepted: 19 September 2025
Published: 10 October 2025

© 2025 Shimizu et al. This work is published and licensed by Dove Medical Press Limited. The full terms of this license are available at https://www.dovepress.com/terms.php and incorporate the Creative Commons Attribution – Non Commercial (unported, v4.0) License (http://creativecommons.org/licenses/by-nc/4.0/). By accessing the work you hereby accept the Terms. Non-commercial uses of the work are permitted without any further permission from Dove Medical Press Limited, provided the work is properly attributed. For permission for commercial use of this work, please see paragraphs 4.2 and 5 of our Terms (https://www.dovepress.com/terms.php).

Recent innovations in digital PET technology have significantly advanced the imaging capabilities for the detection and management of lung cancer. One of the most significant breakthroughs has been the replacement of traditional photomultiplier tubes with digital silicon photomultipliers (SiPMs) with digital displays. This paradigm shift has led to improved spatial and temporal resolution, resulting in better image quality and higher SUVs as compared with conventional analog systems.[5–9] Analog PET/CT shows reduced sensitivity for small lesions and micrometastases due to its limited spatial resolution and lower signal-to-noise ratio. In contrast, digital SiPM technology improves both the spatial and temporal resolution, increases the count rate capability, and enhances lesion detectability, particularly for small node metastases. However, some limitations of these previous reports must be considered including technical validation of digital PET/CT without applying them to NSCLC patients,[5] study of heterogeneous tumor cohorts,[6,7] limited applicability to lung cancer, small sample size,[8] and focus mainly on the system performance rather than on the clinical outcomes.[9]

Several previous studies have systematically compared the results obtained with analog PET versus digital PET systems in oncology patients.[10–12] Firstly, digital PET improves the accuracy of the SUVmax values. The increased count rate leads to a greater reproducibility of SUVmax measurements in digital PET, while the increased contrast resolution makes it easier to differentiate between malignant and benign lesions, even in lesions with low metabolic activity.[10,11] Secondly, with its high resolution and sensitivity, digital PET significantly improves the detection rate of small lesions. In particular, it enables identification of metastases measuring 10 mm or less in diameter, which are often missed by analog PET.[12] Third, digital PET/CT may improve the accuracy of detection of lymph node metastasis. In a previous study, digital PET showed a high sensitivity and moderate-to-high specificity for the detection of cervical node metastasis in patients with head and neck cancer.[13] However, due to the increased sensitivity of this imaging modality, SUVmax values may be elevated even in the presence of inflammation or benign lesions rather than malignancy, increasing likelihood of false-positive results.

Despite these various reports, there are no published studies until date that have compared the performances of digital versus analog PET in patients with NSCLC. In this study, we retrospectively evaluated the diagnostic performance of the two PET/CT modalities in a cohort of patients who had undergone resection for NSCLC. The primary endpoint was comparison of the diagnostic capabilities of the two types of PET/CT for lymph node metastasis, and the secondary endpoints were comparison of the SUVmax values and correlation of the SUVmax values with the tumor Glut-1 (glucose transporter type 1) expression.

Patients and Methods

Study Population

We retrospectively reviewed the data of patients who had undergone surgical resection for NSCLC at our department between August 2022 and July 2024. The inclusion criteria were: (1) primary lung adenocarcinoma or squamous cell carcinoma; (2) tumor diameter between 1–5 cm on CT imaging; (3) FDG-PET/CT imaging performed prior to surgery; (4) histopathological report available. All patients had undergone surgery, while none had received neoadjuvant therapy. The disease TNM stage was evaluated based on of the 8th edition of the American Joint Committee on Cancer TNM Staging Manual.[14] The histopathological diagnoses were determined according to the 2011 IASLC/ATS/ERS classification criteria.[15] Ethics approval for the study was obtained from the Institutional Ethics Committee of Kawasaki Medical School (Approval No. 6650–1).

FDG-PET

Patients underwent PET/CT imaging in either an analog PET/CT scanner or a digital PET/CT scanner. An analog PET/CT scanner (Discovery ST Elite system, GE Healthcare, Japan) was utilized until November 2023, and a digital PET/CT scanner (Cartesion Prime/Luminous Edition system, Canon Medical Systems Corporation, Japan) has been employed since. All patients fasted for at least 4 h before the scan and received intravenous administration of [^{18}F]-FDG (FDG Scan; Nihon Medi-Physics, Tokyo, Japan). An identical FDG dose of 3.7 MBq/kg was administered to all patients, with a fixed uptake time of 60 minutes for both scanners. PET/CT emission scanning was performed one hour after the injection

of [18F]-FDG, following CT data acquisition. The emission time was 2–3 min per bed position, with 5–6 bed positions per patient (head to pelvis). The same reconstruction algorithm (OSEM, iteration × subset, and filter cutoff) was employed across the scanners.

The primary tumors and lymph nodes were analyzed semi-quantitatively based on the SUVmax value, which was defined as the maximum tissue concentration of [18F]-FDG (kBq/mL) in the structure delineated by the region of interest (ROI), divided by the activity injected per gram body weight (kBq/g). The SUVmax was automatically recorded by drawing a rectangular 3-D ROI over the largest area of abnormal [18F]-FDG uptake within the lesion to cover the entire lesion volume. All ROIs were placed by a single experienced nuclear medicine physician under the supervision of a board-certified nuclear medicine specialist. The D/A ratio (digital/analog ratio) was defined as the SUVmax obtained by digital PET/CT divided by the SUVmax obtained by analog PET/CT.

Determination of Lymph Node Metastasis

Final preoperative assessment of lymph node metastasis was performed by a multidisciplinary tumor board, based on an expert radiologist's report. Lymph nodes showing avid [18F]-FDG uptake were considered as being positive for metastasis, except for nodes that showed calcification or bilateral symmetric uptake, and nodes that were not considered as being in the lymphatic drainage pathway. Endobronchial ultrasound-guided transbronchial needle aspiration (EBUS-TBNA) was not routinely performed. Postoperative histopathological assessment of lymph nodes was performed by expert pathologists. The results of this assessment informed subsequent treatment decisions by a multidisciplinary tumor board.

Patients who did not undergo lymph node dissection underwent a CT imaging six months postoperatively and were classified as pN0 if no significant changes were observed. Follow-up information was obtained from the medical records until either disease recurrence or January 31, 2025.

Immunohistochemical Staining

Immunohistochemical analysis was performed using the resected paraffin-embedded lung cancer tissues specimens. After microtome sectioning (4μm), the sections were processed for staining using an automated immunostainer (Nexes; Ventana, Tucson, AZ, USA). The streptavidin-biotin-peroxidase detection technique using diaminobenzidine as the chromogen was applied. The primary antibodies used were accordance with the manufacturer's instructions (Glut-1: 1/200 dilution, clone ab 115730, Abcam). To minimize batch effects, all immunohistochemical stainings were performed using the same antibody lot, and positive/negative controls were included with each run. Tissue sections were stored under controlled humidity and temperature conditions, and sections older than 2 months were not used for this study.

Expression of the marker protein was examined and scored according to a previously reported original protocol. Slides were scored for the intensity of staining (0 to 3) and the percentages of cells with scores of 0(0%), 1(1% to 33%), 2(34% to 66%), and 3(67% to 100%) were determined. The immunohistochemistry (IHC) score (0–9) was defined as the product of the intensity and percentage of cells showing positive staining.[16] The slides were examined by two investigators blinded to the clinicopathological data.

Statistical Analysis

Statistical analysis was performed to examine the significance of differences and possible correlations the clinicopathological features. Fisher's exact test or the χ^2 test was used, as appropriate. To assess the concordance between PET/CT results and histopathological results for lymph nodes, observed agreement was calculated, and Cohen's κ coefficient was used. Wilcoxon's rank-sum test was used to compare continuous data. Pearson's correlation analysis was used to evaluate the correlations between two continuous variables, depending on the normality of the continuous variables. All the statistical analyses were performed using the SPSS software (version 22.0; SPSS Incorporation, Chicago, IL). All statistical tests were two-sided, and probability values of <0.05 were considered as representing statistical significance.

Results

Clinical Characteristics

The patient characteristics are shown in Table 1. Of the 103 patients, 61 patients underwent analog PET/CT, and 42 underwent digital PET/CT. The total patient cohort consisted of individuals ranging in age from 45 to 88 years (mean age: 73.5 years), including 69 men and 34 women. Adenocarcinoma was the predominant histological subtype, identified in 83 patients (80.6%), while squamous cell carcinoma was diagnosed in 20 patients (19.4%). Preoperative assessment identified N0 disease in 90 patients (87.4%), and N1/N2 disease in 13 patients (12.6%). Postoperative pathology identified N0 disease in 88 patients (85.4%) and N1 or N2 disease in 15 patients (14.6%).

SUVmax Values of the Primary Tumors Obtained with the Two Different Scanners

The SUVmax values of the primary tumor in relation to the histological type and tumor size are shown in Table 2 and Figure 1. In a comparison of the characteristics of digital PET/CT and analog PET/CT, notable differences in the D/A ratio were observed across histological subtype and tumor size categories. Higher SUVmax values of the tumors were obtained on digital PET/CT as compared with analog PET in all adenocarcinoma cases (D/A ratio = 2.81, $p < 0.001$), in grade 1 adenocarcinoma cases (D/A ratio = 3.36, $p = 0.125$), in grade 2 adenocarcinoma cases (D/A ratio = 2.50, $p < 0.001$), in grade 3 adenocarcinoma cases (D/A ratio = 3.19, $p = 0.017$), as well as in squamous cell carcinoma cases (D/A ratio = 2.02, $p = 0.009$). The lack of a significant difference in patients with grade 1 adenocarcinoma is likely due to the small number of cases.

Table 1 Patients Characteristics

Characteristics	Digital PET/CT	Analog PET/CT	p-value
Number	42	61	
Age (years)			0.978
Mean	73.5±10.2	73.6±7.1	
Sex			0.713
Male/Female	29/13	40/21	
Histology			0.620
Adenocarcinoma	35	48	
Squamous cell carcinoma	7	13	
Clinical T status			0.999
T1/T2	38/4	54/7	
Clinical N status			0.259
N0/N1/N2	34/6/2	56/4/1	
Clinical Stage			0.181
IA/IB/IIA/IIB/III	31/0/8/3	49/4/7/1	
Type of surgery			0.350
Lobectomy	17	31	
Segmentectomy	10	8	
Wedge	15	22	
Lymph node dissection			0.681
ND2	19	30	
ND1	9	9	
ND0	14	22	
Pathological T status			0.773
T1/T2/T3	31/9/2	47/10/4	
Pathological N status			0.385
N0/N1/N2	35/4/3	53/2/6	
Pathological Stage			0.732
IA/IB/IIA/IIB/III	19/12/6/5	33/12/8/8	

Notes: Categorical variables were compared using the Fisher's exact test or the χ^2 test, and Wilcoxon's rank-sum test was used to compare age.

Table 2 SUVmax of Primary Tumor Across Different Scanners

Characteristics	Digital PET/CT	Analog PET/CT	p-value	D/A Ratio
a) Histological type				
Adenocarcinoma all cases	9.84±8.21	3.50±2.83	<0.001	2.81
Grade 1 cases	3.23±2.16	0.96±0.70	0.125	3.36
Grade 2 cases	8.12±5.56	3.25±2.69	<0.001	2.50
Grade 3 cases	18.78±10.49	5.88±2.60	0.017	3.19
Squamous cell carcinoma	14.78±6.97	7.31±3.95	0.009	2.02
b) Tumor size (clinical T)				
T≤1.0cm	5.94±6.36	1.27±1.36	0.102	4.68
1.0<T≤2.0cm	12.86±10.23	3.76±2.77	0.002	3.42
2.0<T≤3.0cm	11.26±4.38	5.35±3.09	<0.001	2.10
3.0<T≤5.0cm	11.22±10.10	8.59±4.55	0.651	1.31
c) Tumor size (pathological T)				
T≤1.0cm	4.30±5.39	1.28±0.94	0.232	3.36
1.0<T≤2.0cm	11.06±9.71	3.40±2.98	0.009	3.25
2.0<T≤3.0cm	12.53±7.59	5.20±3.07	0.007	2.10
3.0cm<T	13.25±6.17	6.23±4.20	0.002	2.13

Abbreviations: SUV, standardized uptake values; D/A ratio, SUVmax with digital PET/CT divided by that with analog PET/CT. Wilcoxon's rank-sum test was used to compare SUVmax value.

In regard to the SUVmax values versus tumor size in the preoperative CT images, digital PET/CT showed significantly higher SUVmax values as compare with analog PET/CT in tumors measuring 1.1 to 2.0 cm in diameter (D/A ratio = 3.42, p = 0.002) as well as in those measuring 2.1 to 3.0 cm in diameter (D/A ratio = 2.10, p < 0.001); although the sample size was limited and the difference did not reach statistical significance, a 4.48-fold increase was also observed for tumors smaller than 1.0 cm in diameter. However, for tumors exceeding 3.0 cm in diameter, digital PET/CT did not show significantly elevated SUVmax values.

In regard to the SUVmax values versus tumor size as determined by pathological examination, digital PET/CT showed significantly higher SUVmax values as compared with analog PET/CT for tumors measuring 1.1 to 2.0 cm in diameter (D/A ratio = 3.25, p = 0.009), for tumors measuring 2.1 to 3.0 cm in diameter (D/A ratio = 2.10, p =0.007), as well as for tumors exceeding 3.0 cm in diameter (D/A ratio = 2.13, p =0.002). Although the sample size was limited and the difference did not reach statistical significance, a 3.36-fold difference was observed even for tumors smaller than 1.0 cm in diameter. These findings suggest that the performance disparity between digital and analog PET/CT scanners is influenced by the tumor size, with a particularly notable difference observed in tumors smaller than 2.0 cm in diameter. A scatter plot of the primary tumor SUVmax versus pathological tumor size (mm) in NSCLC stratified by the scanner type is shown in Figure 2. Solid lines indicate linear regression fits (Digital PET/CT: $y = 0.12x + 8.34$; Analog PET/CT: $y = 0.11x + 1.7$), and dashed lines show the 95% confidence intervals (CIs).

Correlation Between SUVmax and Tumor Glut-1 Expression

Cohen's Kappa value for interobserver agreement of the measured tumor Glut-1 expression was 0.84. Figure 3 shows the correlation between the SUVmax values and tumor Glut-1 expression in the primary tumors. A significant positive correlation was observed between the tumor Glut-1 expression and SUVmax values in both cases examined by digital PET/CT (r = 0.646, P < 0.001) and analog PET/CT (r = 0.568, P < 0.001). Notably, when the analysis was restricted to tumors measuring 2 cm or less in diameter, the correlation between Glut-1 expression and SUVmax was even more pronounced in the cases examined by digital PET/CT (r = 0.765, P < 0.001) than in analog PET/CT (r = 0617, P < 0.001). The correlation coefficient was, however, higher in the cases examined by digital PET, particularly for tumors measuring less than 2 cm in diameter.

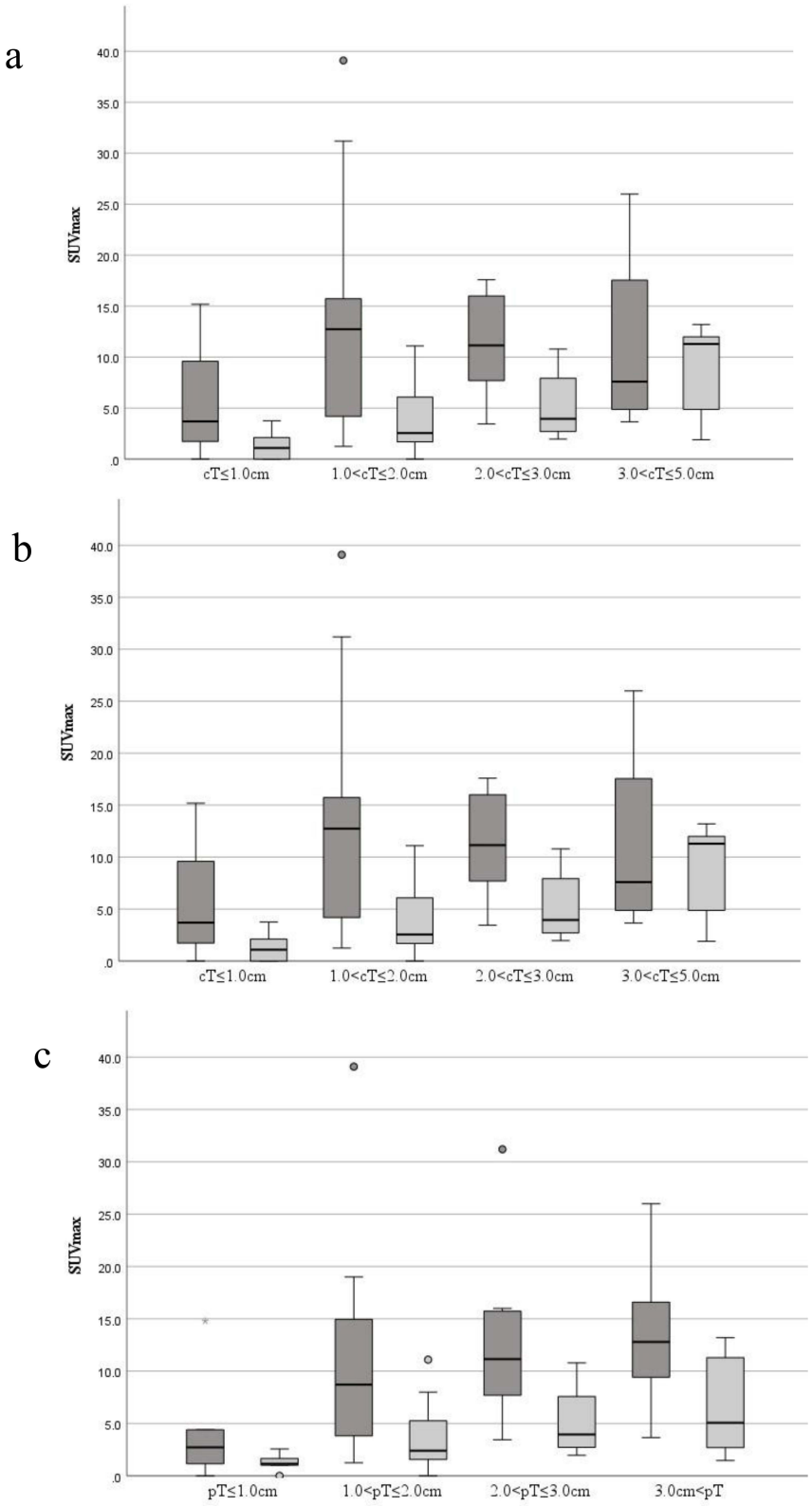

Figure 1 The SUVmax values of the primary tumor according to histological type and tumor size. (**a**) Distribution of SUVmax by histological type. (**b**) Relationship between SUVmax and tumor diameter measured on CT. (**c**) Relationship between SUVmax and tumor diameter measured on pathological specimens. Boxes represent the interquartile range (IQR), whiskers indicate the minimum and maximum within 1.5×IQR, and horizontal lines within the boxes indicate the median.

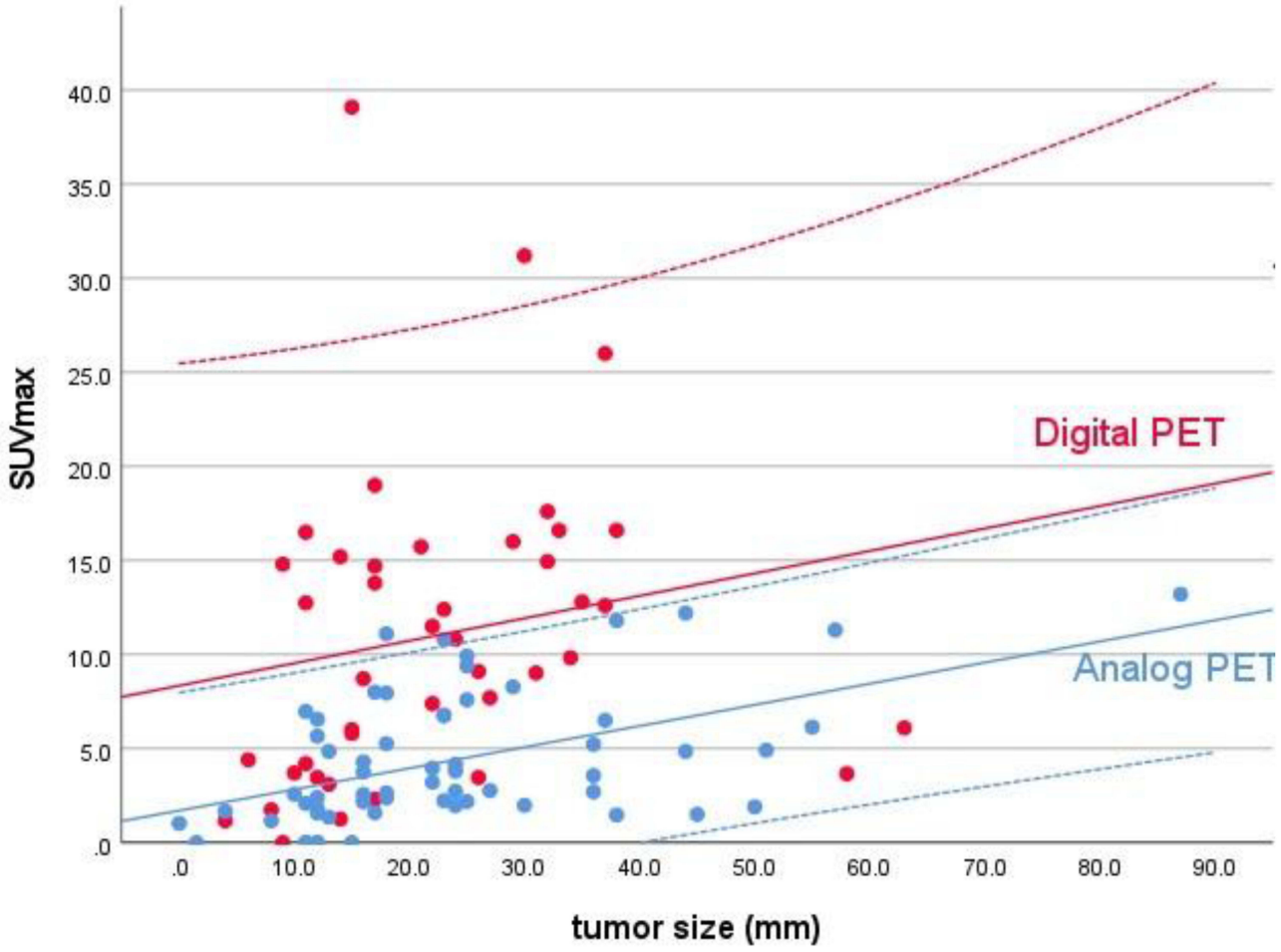

Figure 2 Scatter plot of primary tumor SUVmax versus pathological tumor size (mm) in NSCLC, stratified by scanner type. Red circles = digital PET/CT; blue circles = analog PET/CT. Solid lines indicate linear regression fits (Digital PET/CT: y = 0.12x + 8.34; Analog PET/CT: y = 0.11x + 1.7), and dashed lines show the 95% confidence intervals.

Diagnostic Performance for the Two Types of Scanners for Metastatic Lymph Nodes

We then assessed the diagnostic performance of the two types of scanners for metastatic lymph nodes. The sensitivity, specificity, positive predictive value (PPV), negative predictive value (NPV), and accuracy of PET/CT are shown in Table 3 for all cases and in Table 4 for cases with pathological diagnoses following lymph node dissection. In the overall subject populations, digital PET/CT showed a sensitivity of 71.4% (95% CI: 29.0–95.7%), specificity of 88.6% (95% CI: 73.3–97.2%), and accuracy of 85.7% (95% CI: 70.9–94.7%) for the diagnosis of lymph node metastasis. The PPV was 55.6% (95% CI: 21.3–86.1%), while the NPV was 93.9% (95% CI: 78.9–99.3%). Cohen's κ was 0.539, indicating moderate agreement. On the other hand, analog PET/CT showed a sensitivity of 37.5% (95% CI: 9.4–75.3%), specificity of 96.2% (95% CI: 85.1–99.8%), and accuracy of 88.5% (95% CI: 76.9–95.7%). The PPV was 60.0% (95% CI: 14.7–94.7%), while the NPV was 91.1% (95% CI: 80.2–97.0%). Cohen's κ was 0.401, indicating moderate agreement. As compared with analog PET/CT, the sensitivity of digital PET/CT was twofold higher, but the specificity was slightly lower, and there was no difference in the accuracy (Table 3).

In patients with histopathological diagnosis of lymph node metastasis, a sensitivity of digital PET/CT was 66.7% (95% CI: 22.3–95.7%), specificity was 81.8% (95% CI: 59.7–94.8%), and accuracy was 78.6% (95% CI: 59.0–91.7%). The PPV was 50.0% (95% CI: 15.7–84.3%), while the NPV was 90.0% (95% CI: 68.3–98.8%). Cohen's κ was 0.434, indicating moderate agreement. On the other hand, in these patients, analog PET/CT showed a sensitivity of 37.5% (95% CI: 8.5–75.5%), specificity of 93.5% (95% CI: 78.6–99.2%), and accuracy of 82.1% (95% CI: 66.5–92.5%). The PPV

a

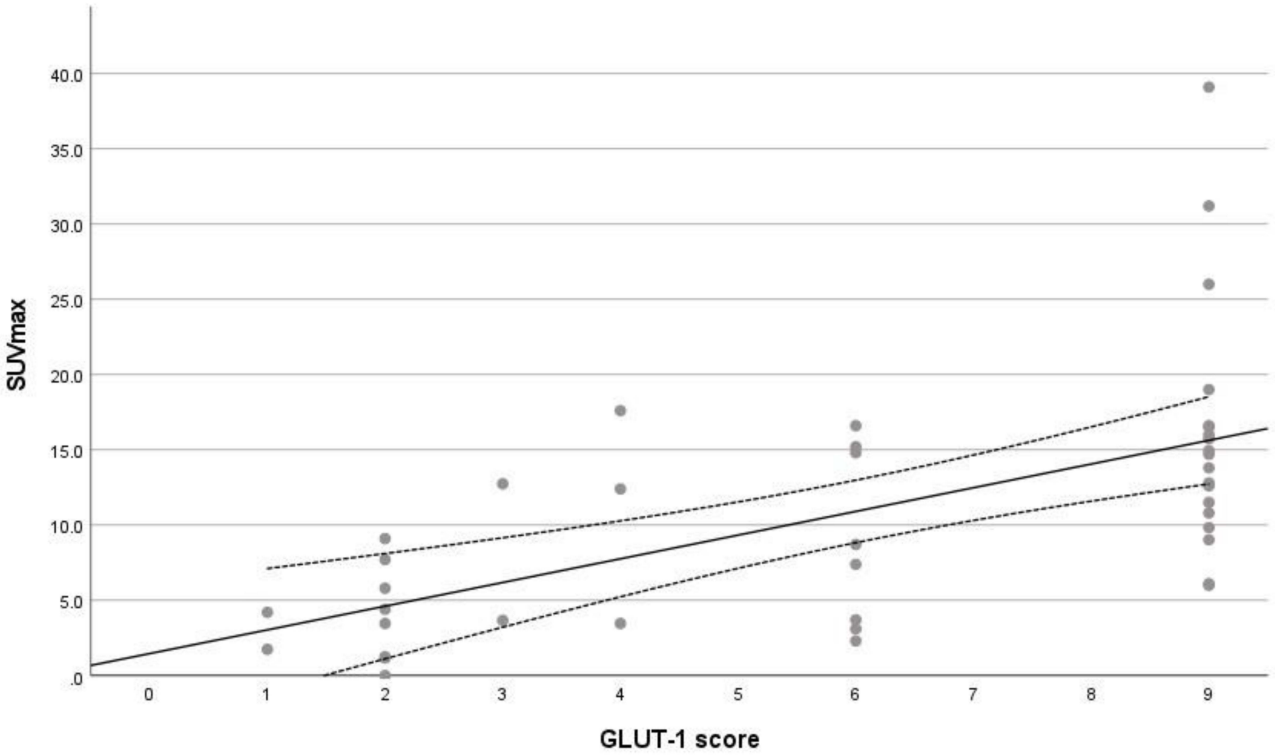

b

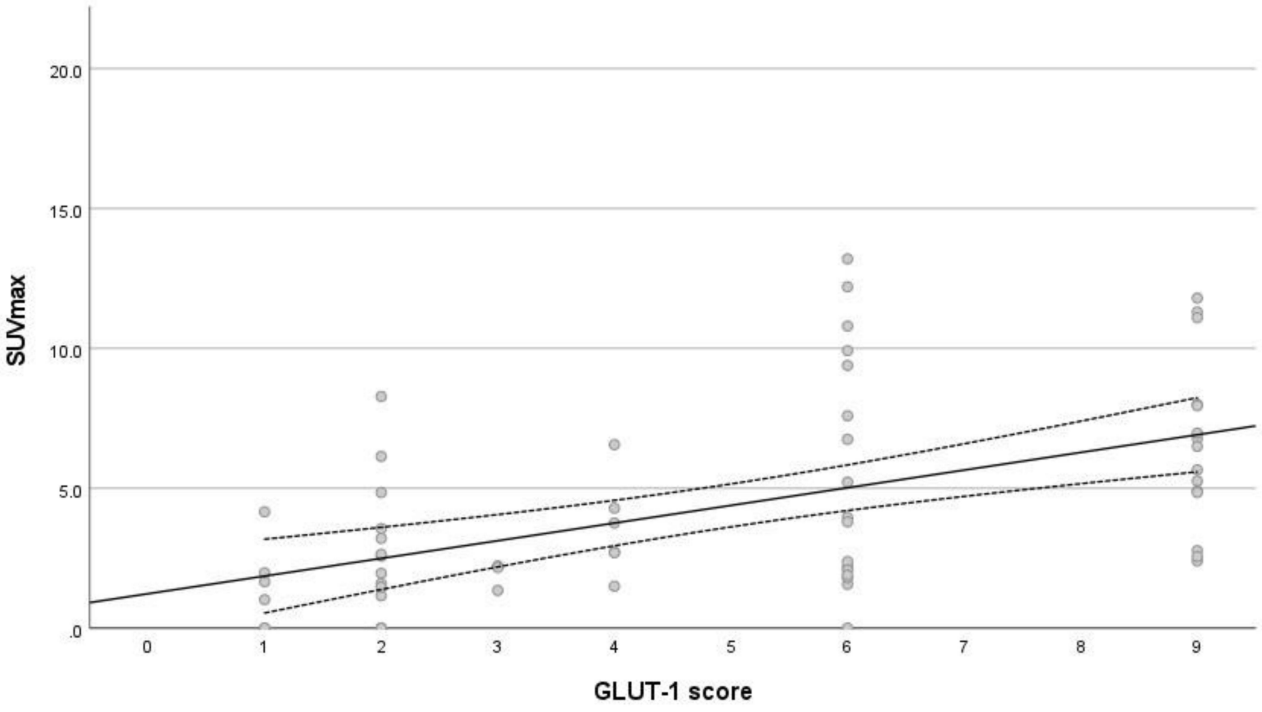

Figure 3 Continued.

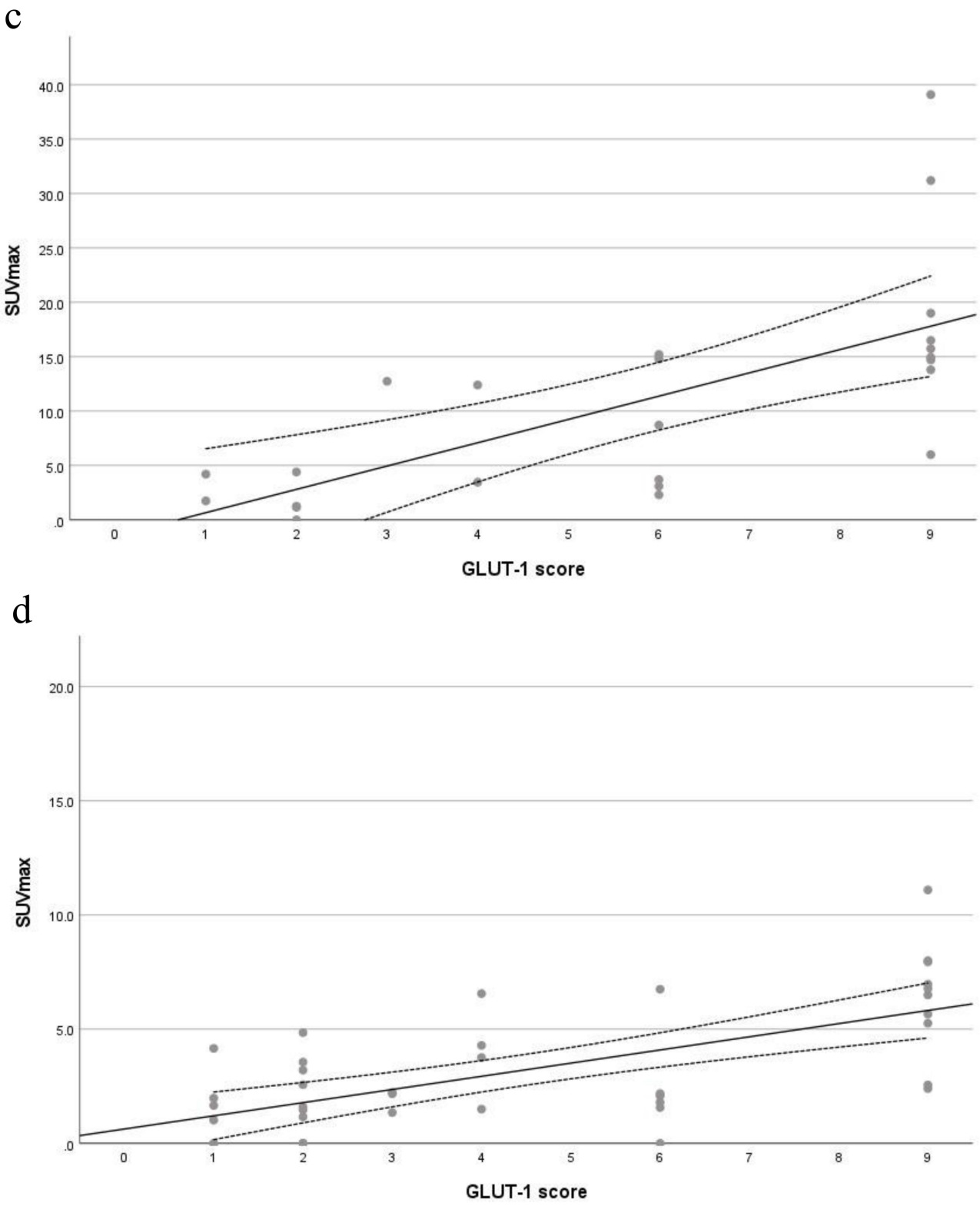

Figure 3 Linear regression analysis Linear regression analysis showed a significant positive correlation, overall, between the tumor Glut-1 expression and the SUVmax in both cases examined by digital PET/CT (Figure 1a; r = 0.646, P < 0.001) and those examined by analog PET/CT (Figure 1b; r = 0.568, P < 0.001). When the analysis was restricted to tumors measuring 2 cm or less in diameter, the correlation was even more pronounced in the cases examined by digital PET/CT (Figure 1c; r = 0.765, P < 0.001) than in analog PET/CT (Figure 1d; r = 0617, P < 0.001).

https://doi.org/10.2147/CMAR.S542593

Table 3 Diagnostic Performance for Metastatic Lymph Nodes Across Different Scanners in All Cases

		Postoperative diagnosis		Total
		Positive	Negative	
a) Digital PET/CT, Cohen's κ =0.539				
Preoperative diagnosis	Positive	5	4	9
	Negative	2	31	33
Total		7	35	42
Sensitivity: 71.4% (95% CI:0.290–0.957)				
Specificity: 88.6% (95% CI:0.733–0.972)				
Accuracy: 85.7% (95% CI:0.709–0.947)				
PPV: 55.6% (95% CI:0.213–0.861)				
NPV: 93.9% (95% CI:0.789–0.993)				
b) Analog PET/CT, Cohen's κ =0.401				
Preoperative diagnosis	Positive	3	2	5
	Negative	5	51	56
Total		8	53	61
Sensitivity: 37.5% (95% CI:0.094–0.753)				
Specificity: 96.2% (95% CI:0.851–0.998)				
Accuracy: 88.5% (95% CI:0.769–0.957)				
PPV: 60.0% (95% CI:0.147–0.947)				
NPV: 91.1% (95% CI:0.802–0.970)				

Notes: Cohen's κ coefficient was calculated to assess agreement between PET/CT and pathology.
Abbreviations: PPV, positive predictive value; NPV, negative predictive value.

was 60.0% (95% CI: 14.7–94.7%), while the NPV was 85.3% (95% CI: 66.5–95.5%). Cohen's κ was 0.363, indicating moderate agreement. As compared with analog PET, the sensitivity of digital PET/CT was twofold higher, but the specificity was slightly lower, and there was no difference in the accuracy (Table 4).

Characteristics of Each Lymph Node in Digital PET/CT

Figure 4 shows examples of digital PET/CT imaging, hematoxylin-eosin (HE) staining, and Glut-1 expression in the primary tumors and lymph nodes. Case A was a true-positive case; this patient was a 61-year-old woman with pulmonary cT1cN1M0 papillary adenocarcinoma of the left upper lobe. Case B was a false-negative case; the patient was a 76-year-old man with pulmonary cT1cN0M0 papillary adenocarcinoma of the right lower lobe. Case C was a false-positive case; the patient was an 87-year-old man with pulmonary cT1cN0M0 papillary adenocarcinoma of the right upper lobe. Case D was another false-positive case; this patient was a 79-year-old man with pulmonary cT1aN0M0 acinar adenocarcinoma of the right upper lobe.

Table 5 shows the characteristics of each case and of the lymph nodes evaluated by digital PET/CT. Specifically, among the false-negative cases (n = 4), 2 patients (50%) had micrometastases, and 2 cases (50%) showed low tumor

Table 4 Diagnostic Performance for Metastatic Lymph Nodes Across Different Scanners in Patients with Dissection or Sampling

		Postoperative diagnosis		Total
		Positive	Negative	
a) Digital PET/CT, Cohen's κ =0.434				
Preoperative diagnosis	Positive	4	4	8
	Negative	2	18	20
Total		6	22	28
Sensitivity: 66.7% (95% CI:0.223–0.957)				
Specificity: 81.8% (95% CI:0.597–0.948)				
Accuracy: 78.6% (95% CI:0.590–0.917)				
PPV: 50.0% (95% CI:0.157–0.843)				
NPV: 90.0% (95% CI:0.683–0.988)				
b) Analog PET/CT, Cohen's κ =0.363				
Preoperative diagnosis	Positive	3	2	5
	Negative	5	29	34
Total		8	31	39
Sensitivity: 37.5% (95% CI:0.085–0.755)				
Specificity: 93.5% (95% CI:0.786–0.992)				
Accuracy: 82.1% (95% CI:0.665–0.925)				
PPV: 60.0% (95% CI:0.147–0.947)				
NPV: 85.3% (95% CI:0.665–0.955)				

Note: Cohen's κ coefficient was calculated to assess agreement between PET/CT and pathology.
Abbreviations: PPV, positive predictive value; NPV, negative predictive value.

Glut-1 expression. As compared with the true-positive cases, the false-positive lymph nodes tended to show lower SUVmax values (primary tumor: 15.40 vs 7.73, p = 0.078; lymph node: 7.88 vs 5.10, p = 0.105). Among the false-positive lymph nodes, two showed evidences of pneumoconiosis, while the others showed evidence of anthracosis or granuloma; all showed high Glut-1 expression scores.

Discussion

In recent years, there have been significant advances in the perioperative treatment of lymph node-positive lung cancer, particularly in respect of optimization of the preoperative treatment strategies, that have contributed to improved outcomes.[17,18] Therefore, accurate lymph node assessment is essential for determining the appropriate treatment strategy and for predicting the prognosis. FDG-PET/CT has a profound impact on the treatment decisions in patients with malignant tumors. According to a multicenter study, the findings of PET/CT significantly influenced subsequent therapeutic strategies in 71.6% of lung cancer cases.[19] PET/CT is reported to show as sensitivity of 70%, specificity of 94%, PPV of 64%, and NPV of 94% for the detection of lymph node metastases in lung cancer.[20] In our subject who had been imaged in a digital PET/CT scanner, the sensitivity and specificity for patient-based nodal staging were 71%

and 88%, respectively. These values were similar to the pooled estimates for conventional PET/CT. Differences likely reflect (i) adoption-phase protocol optimization and reader calibration; (ii) reconstruction choice and version influencing lesion SUV/noise; (iii) harmonization status across software updates; and (iv) biology/prevalence (small-volume disease, granulomatous background).[21]

In our study, false-positive results were obtained in several cases examined by digital PET/CT. On histopathological evaluation, the lymph nodes in these cases frequently contained evidence of anthracosis, pneumoconiosis, or granulomatous inflammation without malignancy. These findings are consistent with previous reports. For example, Shiraki et al demonstrated that false-positive FDG uptake in the hilar and mediastinal lymph nodes was mainly attributable to benign conditions such as chronic inflammation and dust-related lung disease, including anthracosis and other pneumoconioses.[22] Similarly, Lee et al investigated NSCLC patients in a country where tuberculosis is endemic and found that false-positive PET/CT results were frequently obtained in patients with inflammatory granulomas, particularly of tuberculous origin. Importantly, they showed that taking into account the morphological features of the lymph nodes, such as presence/absence

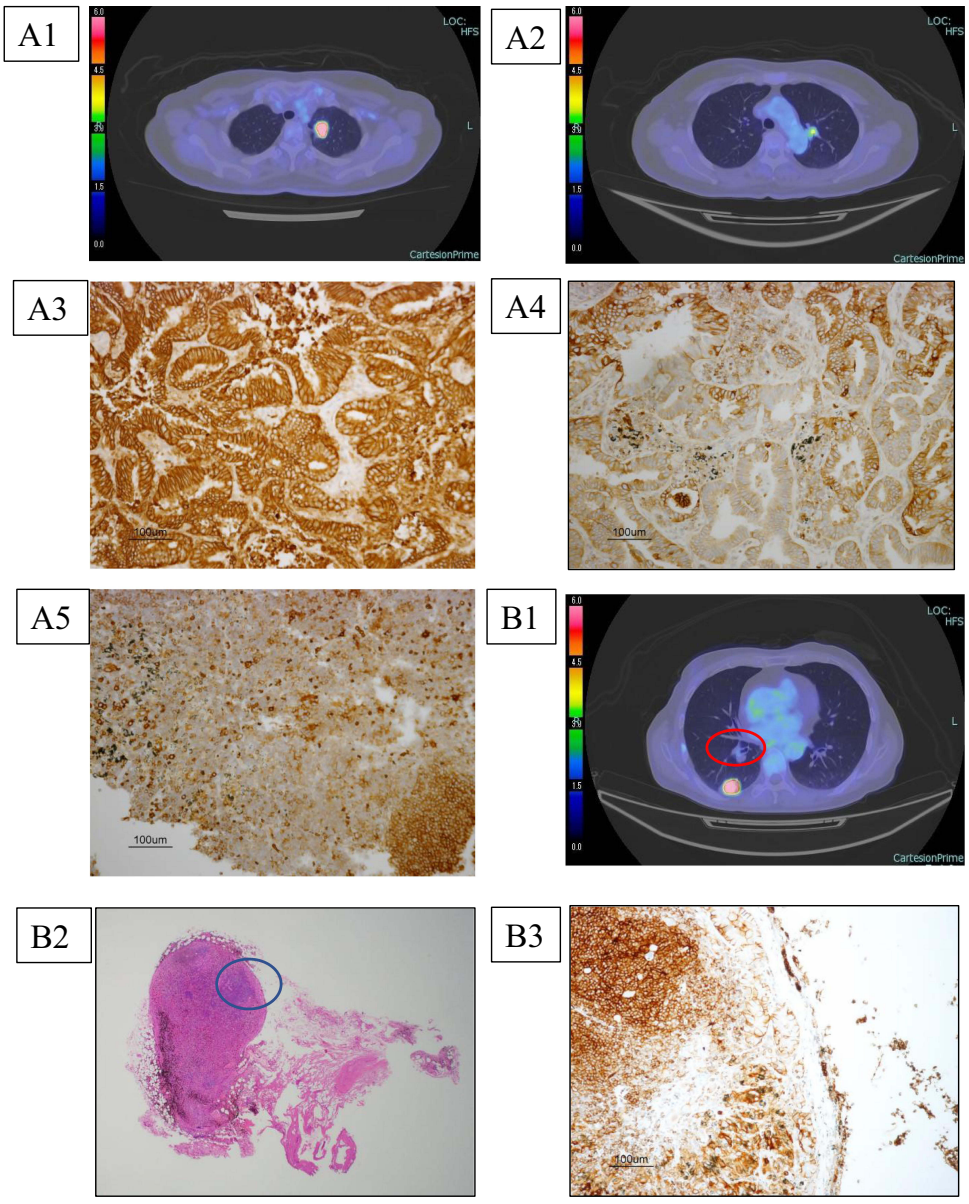

Figure 4 Continued.

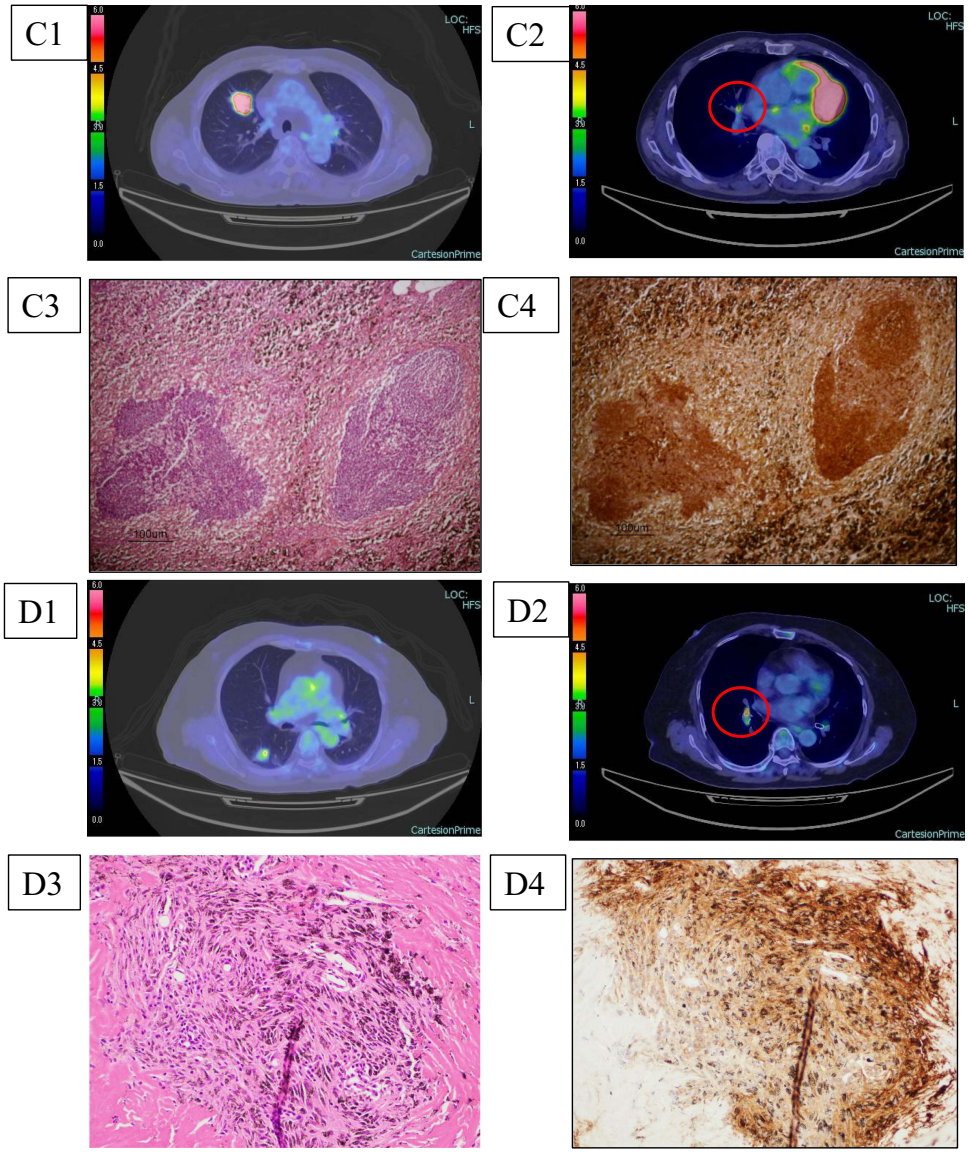

Figure 4 Representative cases (**A**) True-positive and false-negative case. (**A**) 61-year-old woman with papillary adenocarcinoma. The primary tumor showed SUVmax of 16.00 and the hilar lymph node showed SUVmax of 4.22. (**A1** and **A2**) Pathological analysis showed hilar and mediastinal lymph node metastasis. The Glut-1 expression score of the primary tumor was 9 (**A3**), while the score of the mediastinal lymph node was 1(**A4**), and that of the hilar lymph node is 2 (**A5**). (**B**): False-negative case. A 76-year-old man with papillary adenocarcinoma. The primary tumor showed SUVmax of 16.60 and the hilar lymph node showed no FDG uptake (**B1** red circle). Pathological analysis revealed hilar lymph node metastasis. Micrometastasis was identified by HE staining (**B2** blue circle), and the Glut-1 expression score was 4 (**B3**). (**C**): False-positive case. An 87-year-old man with papillary adenocarcinoma. The primary tumor showed SUVmax of 17.60 (**C1**), while the hilar lymph node showed SUVmax of 5.50 (**C2** red circle). HE staining of this lymph node showed pneumoconiosis (**C3**), and the Glut-1 expression score was 6 (**C4**). (**D**): False-positive case. A 79-year-old man with acinar adenocarcinoma. The primary tumor showed SUVmax of 4.40 (**D1**), and the lymph node showed an SUVmax of 5.40 (**D2** red circle). HE staining of this lymph node showed anthracosis (**D3**), and the Glut-1 expression score was 4 (**D4**).

of calcification and distribution patterns along the lymphatic drainage pathways could improve the diagnostic specificity.[23] To minimize false-positives, lymph nodes showing calcifications, symmetrical lymph nodes findings and positive finding in lymph nodes not aligned along the lymphatic drainage pathway should not be classified as metastases.[23,24] Conversely, false-negative results are primarily attributed to the limited spatial resolution of PET, particularly for detecting micro-metastases with a minimal tumor burden. Despite this understanding, comprehensive studies addressing the spatial resolution limitations in such cases are still lacking.[20] Digital PET/CT provides sensitive and high-resolution imaging and has the potential to improve the detection accuracy of small lymph node metastases as compared with conventional

Table 5 Characteristics in Each Cases and Lymph Nodes in Digital PET/CT

Case	Histology (Grade)	Background of Lung	Location	SUVmax		LN Pathology		Glut-1 Expression	
				TM	LN			TM	LN
a) True positive cases									
1	Ad (G2)	Normal	4R	13.80	10.70	Metastasis	TP	9	9
			11s		-	Metastasis	FN		2
2	Sq	Normal	12	19.00	8.10	Metastasis	TP	9	9
3	Ad (G2)	Normal	5	16.00	-	Metastasis	FN	9	1
			13		4.22	Metastasis	TP		6
4	Ad (G2)	Normal	6	12.80	8.50	Metastasis	TP	9	6
b) False negative cases									
5	Ad (G3)	Normal	12	16.60	-	Micro metastasis	FN	9	2
6	Ad (G3)	Normal	10	11.50	-	Micro metastasis	FN	6	1
c) False positive cases									
7	Ad (G2)	Normal	12	17.60	5.50	Pneumoconiosis	FP	4	6
8	Ad (G2)	Asthma	11s	4.40	5.40	Anthracosis	FP	2	4
9	Ad (G2)	Fibrosis	11s	3.10	3.50	Granuloma	FP	6	4
10	Ad (G1)	Pneumoconiosis	11i	5.80	6.00	Pneumoconiosis	FP	2	4

Abbreviations: TP, true positive; FN, false negative; FP, false positive; Sq, squamous cell carcinoma; Ad, adenocarcinoma; TM, primary tumor; LN, lymph node.

PET/CT. This technological advancement may enable more accurate diagnosis of lymph node metastases and contribute to selection of the optimal treatment strategy for each patient. Furthermore, accurate lymph node diagnosis is expected to improve the quality of life of the patients by allowing avoidance of overtreatment and preventing inadequate treatment.

This study demonstrated that digital PET/CT is a highly valuable modality for predicting the presence of intrathoracic lymph node metastases as compared with analog PET/CT. In particular, digital PET/CT shows a twofold higher sensitivity for the detection of lymph node metastasis as compared with analog PET/CT. Although the specificity was slightly reduced, there was no statistically significant difference in the overall diagnostic accuracy. In this study, all the false-negative cases had micrometastases, an inherent limitation of tumor detection by FDG-PET imaging. In addition, digital PET/CT was superior to analog PET/CT for early detection of small lesions.

While the advantages of this "next generation" PET modality have been elucidated, several considerations need to be addressed in the transition from analog to digital PET systems. Key issues for future application include the potential divergence in the reference ranges for SUVmax values as compared with those in conventional analog PET, which will require a comprehensive re-evaluation of the diagnostic cut-off thresholds. In addition, inconsistencies in SUVmax measurements between digital and analog systems may lead to deviations from established diagnostic standards.[7] Consequently, accumulation of further clinical experience and continued advancement of physician expertise are imperative to ensure precise interpretation and effective application of digital PET findings.

The results of immunostaining with Glut-1 showed a stronger correlation between the SUV values and tumor Glut-1 expression in cases scanned by digital PET/CT than in those scanned by analog PET, especially for tumors measuring less than 2 cm in diameter. The SUV value is a widely used utilized parameter for evaluating the metabolic activity, particularly in tumors, in FDG-PET. This is because FDG, a glucose analog, is actively taken up by cells with elevated metabolic rates. Consequently, SUV values quantitatively reflect the extent of metabolic activity in tumor tissues and are instrumental in the diagnosis, assessment of the prognosis and evaluation of the treatment efficacy.[25,26] Glut-1 facilitates glucose transport across the cell membrane and plays a pivotal role in glucose uptake within tumor cells. In malignant tumors, Glut-1 expression is upregulated due to the Warburg effect, which sustains elevated glucose metabolism irrespective of oxygen availability.[27,28] Thus, Glut-1 expression also serves as a biomarker of tumor glucose uptake capacity and metabolic activity. There is evidence to suggest that the SUV values in FDG-PET are correlated with the Glut-1 expression levels, as both reflect the degree of metabolic activity. Specifically, tumors exhibiting high Glut-1 expression often showed increased FDG uptakes and thereby, higher SUV values. This relationship may also underlie the observed correlation among the Glut-1 expression levels, the SUV values, tumor grade, and clinical prognosis. Tumors with elevated SUV values and Glut-1 expression are typically more aggressive and associated with a poorer prognosis.[29–31] Moreover, tumors with elevated Glut-1 expression levels may exhibit greater sensitivity to metabolic therapies targeting glucose metabolism (eg, glucose metabolism inhibitors). Understanding the interplay between SUV values and Glut-1 expression could enhance our knowledge of the tumor metabolic pathophysiology and foster the development of novel therapeutic strategies. Collectively, these findings, alongside the assessment of SUV values and Glut-1 expression, may yield a more nuanced characterization of tumor biology and facilitate the optimization of individualized treatment strategies for patients.

This study had several limitations that should be considered when interpreting the results. First, it was a single-center and retrospective study conducted in a small selected patient group. The sample size was determined based on all available cases during the study period. Therefore, a priori calculation of the target sample size could not be performed. For subgroups with a small sample size, non-parametric tests were applied. However, it should be noted that the statistical power is limited in such small samples, and the interpretation should be considered exploratory rather than confirmatory. Second, in the early phase of introduction of digital PET, there is inevitably a potential learning curve effect in interpretation, which could have influenced the results. Third, our findings are limited to a Japanese cohort and two specific scanner models. To improve the generalizability of the results, future multicenter studies across different ethnic groups and scanner platforms are necessary.

We proposed preliminary recalibration of the SUVmax thresholds for digital PET/CT for NSCLC. Based on our data, the D/A SUVmax ratio suggest that conventional cutoffs may underestimate positivity in digital PET. Further clinical trials are necessary to determine the appropriate thresholds. These trials should include standardized acquisition protocols

used across multiple digital PET/CT systems, prospective validation of the SUVmax cutoff values, and integration of a histopathological gold standard. Inclusion of the above in the study design could improve the clinical workflow and establish robust SUVmax thresholds for digital PET/CT.

Conclusions

In this study, digital PET/CT showed a twofold higher sensitivity as compared with analog PET/CT for the diagnosis of lymph node metastasis (71.4% vs 37.5%), while maintaining comparable accuracy (85.7% vs 88.5%). Digital PET/CT showed better diagnostic sensitivity, with higher SUV values, than analog PET/CT, especially for lesions smaller than 2 cm in diameter, and the SUV values tends to show a stronger correlation with the Glut-1 expression. While digital PET shows superior ability to detect lymph node metastases and small lesion in cases of NSCLC and also an improved accuracy of the SUVmax, the relatively high false-positive remains a challenge. Therefore, future multicenter prospective studies and a standardized redefinition of SUVmax are urgently needed to validate our findings and to for more reliable clinical application of digital PET/CT in patients with lung cancer.

Data Sharing Statement

The data is not publicly available to protect patient privacy. Further details and other data supporting our study's findings are available from the corresponding author upon reasonable request.

Ethics Approval and Informed Consent

All procedures were performed in accordance with the Helsinki Declaration and were reviewed and approved by the Ethics Committee of the Kawasaki medical school. This study was conducted retrospectively, and some patients were deceased at the commencement of the study. Our data did not contain any personally identifiable patient information and underwent confidentiality measures during the data collection process. Due to these aforementioned factors, the need for written informed consent was waived by the ethics committee of the Kawasaki medical school.

Acknowledgment

The authors thank Keiko Isoda (Kawasaki Medical School) for providing technical assistance. The Authors would like to thank IMIC (http://www.imic.or.jp/) for the English language review.

Consent for Publication

All authors agreed to publish the paper in any form.

Funding

This work was supported by JSPS KAKENHI Grant Number JP25K12117, and Research Project Grant NO. R06B-090 from Kawasaki Medical School.

Disclosure

The authors declare no conflicts of interest in this work.

References

1. Ung YC, Maziak DE, Vanderveen JA, et al. ^{18}Fluorodeoxyglucose positron emission tomography in the diagnosis and staging of lung cancer: a systematic review. *J Natl Cancer Inst*. 2007;99(23):1753–1767. doi:10.1093/jnci/djm232
2. Vansteenkiste JF, Stroobants SG, Dupont PJ, et al. Prognostic importance of the standardized uptake value on ^{18}f-fluoro-2-deoxy-glucose–positron emission tomography scan in non–small-cell lung cancer: an analysis of 125 cases. *J Clin Oncol*. 1999;17(10):3201–3206. doi:10.1200/JCO.1999.17.10.3201
3. Nomori H, Watanabe K, Ohtsuka T, et al. Fluorine 18-tagged fluorodeoxyglucose positron emission tomographic scanning to predict lymph node metastasis, invasiveness, or both, in clinical T1 N0 M0 lung adenocarcinoma. *J Thorac Cardiovasc Surg*. 2004;128(3):396–401. doi:10.1016/j.jtcvs.2004.03.020
4. Cerfolio RJ, Bryant AS, Ohja B, et al. The maximum standardized uptake values on positron emission tomography of a non-small cell lung cancer predict stage, recurrence, and survival. *J Thorac Cardiovasc Surg*. 2005;130(1):151–159. doi:10.1016/j.jtcvs.2004.11.007

5. Hsu DF, Ilan E, Peterson WT, Uribe J, Lubberink M, Levin CS. Studies of a next generation silicon-photomultiplier–based time-of-flight PET/CT system. *J Nucl Med*. 2017;58(9):1511–1518. doi:10.2967/jnumed.117.189514
6. Koopman D, van Dalen JA, Stevens H, et al. Performance of digital PET compared to high-resolution conventional PET in patients with cancer. *J Nucl Med*. 2020;61(10):1448–1454. doi:10.2967/jnumed.119.238105
7. Fuentes-Ocampo F, López-Mora DA, Flotats A, et al. Digital vs. analog PET/CT: intra-subject comparison of the SUVmax in target lesions and reference regions. *Eur J Nucl Med Mol Imaging*. 2019;46(5):1204. doi:10.1007/s00259-019-04280-0
8. Chen X, Hu P, Yu H, et al. Head-to-head intra-individual comparison of total-body 2-[18F] FDG PET/CT and digital PET/CT in patients with malignant tumor: how sensitive could it be? *Eur Radiol*. 2023;33(11):7890–7898. doi:10.1007/s00330-023-09825-4
9. van Sluis J, de Jong J, Schaar J, et al. Performance characteristics of the digital Biograph Vision PET/CT system. *J Nucl Med*. 2019;60(7):1031–1036. doi:10.2967/jnumed.118.215418
10. de Jong TL, Koopman D, van Dalen JA, et al. Performance of digital PET/CT compared with conventional PET/CT in oncologic patients: a prospective comparison study. *Ann Nucl Med*. 2022;36(8):756–764. doi:10.1007/s12149-022-01758-0
11. Nguyen NC, Vercher-Conejero J, Sattar A, et al. Image quality and diagnostic performance of a digital PET prototype in patients with oncologic diseases: initial experience and comparison with analog PET. *J Nucl Med*. 2015;56(9):1378–1385. doi:10.2967/jnumed.114.148338
12. López-Mora DA, Flotats A, Fuentes-Ocampo F, et al. Comparison of image quality and lesion detection between digital and analog PET/CT. *Eur J Nucl Med Mol Imaging*. 2019;46(6):1383–1390. doi:10.1007/s00259-019-4260-z
13. Butt F, Dominguez-Konicki L, Tocci N, Paydarfar J, Seltzer M, Pastel D. Diagnostic accuracy of the latestgeneration digital PET/CT scanner for detection of metastatic lymph nodes in head and neck cancer. *Front Nucl Med*. 2023;30:1184448. doi:10.3389/fnume.2023.1184448
14. Goldstraw P, Chansky K, Crowley J, et al. The IASLC lung cancer staging project: proposals for revision of the TNM stage groupings in the forthcoming (Eighth) edition of the TNM Classification for lung cancer. *J Thorac Oncol*. 2016;11(1):39–51. doi:10.1016/j.jtho.2015.09.009
15. Travis WD, Brambilla E, Noguchi M, et al. International association for the study of lung cancer/American thoracic society/european respiratory society international multidisciplinary classification of lung adenocarcinoma. *J Thorac Oncol*. 2011;6(2):244–285. doi:10.1097/JTO.0b013e318206a221
16. Taira N, Atsumi E, Nakachi S, et al. Comparison of GLUT-1, SGLT-1, and SGLT-2 expression in false-negative and true-positive lymph nodes during the ^{18}F-FDG PET/CT mediastinal nodal staging of non-small cell lung cancer. *Lung Cancer*. 2018;123:30–35. doi:10.1016/j.lungcan.2018.06.004
17. Forde PM, Spicer J, Lu S, et al. Neoadjuvant nivolumab plus chemotherapy in resectable lung cancer. *N Engl J Med*. 2022;386(21):1973–1985. doi:10.1056/NEJMoa2202170
18. Spicer JD, Garassino MC, Wakelee H, et al. Neoadjuvant pembrolizumab plus chemotherapy followed by adjuvant pembrolizumab compared with neoadjuvant chemotherapy alone in patients with early-stage non-small-cell lung cancer (KEYNOTE-671): a randomised, double-blind, placebo-controlled, Phase 3 trial. *Lancet*. 2024;404(10459):1240–1252. doi:10.1016/S0140-6736(24)01756-2
19. Kubota K, Matsuno S, Morioka N, et al. Impact of FDG-PET findings on decisions regarding patient management strategies: a multicenter trial in patients with lung cancer and other types of cancer. *Ann Nucl Med*. 2015;29(5):431–441. doi:10.1007/s12149-015-0963-9
20. Kitajima K, Doi H, Kanda T, et al. Present and future roles of FDG - PET/CT imaging in the management of lung cancer. *Jpn J Radiol*. 2016;34(6):387–399. doi:10.1007/s11604-016-0546-2
21. Lindström E, Sundin A, Trampal C, **et.al**. evaluation of penalized-likelihood estimation reconstruction on a digital time-of-Flight PET/CT Scanner for ^{18}F-FDG whole-body examinations. *J Nucl Med*. 2018;59(7):1152–1158. PMID: 29449445. doi:10.2967/jnumed.117.200790
22. Shiraki N, Hara M, Ogino H, et al. False-positive and true-negative hilar and mediastinal lymph nodes on FDG-PET–radiological-pathological correlation. *Ann Nucl Med*. 2004;18(1):23–28. doi:10.1007/BF02985610
23. Lee JW, Kim BS, Lee DS, et al. 18F-FDG PET/CT in mediastinal lymph node staging of non-small-cell lung cancer in a tuberculosis-endemic country: consideration of lymph node calcification and distribution pattern to improve specificity. *Eur J Nucl Med Mol Imaging*. 2009;36(11):1794–1802. doi:10.1007/s00259-009-1155-4
24. Shigemoto Y, Suga K, Matsunaga N. F-18-FDG-avid lymph node metastasis along preferential lymphatic drainage pathways from the tumor-bearing lung lobe on F-18-FDG PET/CT in patients with non-small-cell lung cancer. *Ann Nucl Med*. 2016;30(4):287–297. doi:10.1007/s12149-016-1063-1
25. Vesselle H, Freeman JD, Wiens L, et al. Fluorodeoxyglucose Uptake of primary non-small cell lung cancer at positron emission tomography: new contrary data on prognostic role. *Clin Cancer Res*. 2007;13(11):3255–3263. doi:10.1158/1078-0432.CCR-06-1128
26. Paesmans M, Berghmans T, Dusart M, et al. Primary tumor standardized uptake value measured on fluorodeoxyglucose positron emission tomography is of prognostic value for survival in non-small cell lung cancer. *J Thorac Oncol*. 2010;5(5):612–619. doi:10.1097/JTO.0b013e3181d0a4f5
27. Ganapathy V, Thangaraju M, Prasad PD. Nutrient transporters in cancer: relevance to Warburg hypothesis and beyond. *Pharmacol Ther*. 2009;121(1):29–40. doi:10.1016/j.pharmthera.2008.09.005
28. Koppenol WH, Bounds PL, Dang CV. Otto Warburg's contributions to current concepts of cancer metabolism. *Nat Rev Cancer*. 2011;11(5):325–337. doi:10.1038/nrc3038
29. Kurata T, Oguri T, Isobe T, Ishioka S, Yamakido M. Differential expression of facilitative glucose transporter (GLUT) genes in primary lung cancers and their liver metastases. *Jpn J Cancer Res*. 1999;90(11):1238–1243. doi:10.1111/j.1349-7006.1999.tb00702.x
30. Taylor MD, Smith PW, Brix WK, et al. Fluorodeoxyglucose positron emission tomography and tumor marker expression in non-small cell lung cancer. *J Thorac Cardiovasc Surg*. 2009;137(1):43–48. doi:10.1016/j.jtcvs.2008.10.014
31. Chung JH, Lee WW, Park SY, et al. FDG uptake and glucose transporter type 1 expression in lymph nodes of non-small cell lung cancer. *Eur J Surg Oncol*. 2006;32(9):989–995. doi:10.1016/j.ejso.2006.05.017

Cancer Management and Research

Dovepress
Taylor & Francis Group

Publish your work in this journal

Cancer Management and Research is an international, peer-reviewed open access journal focusing on cancer research and the optimal use of preventative and integrated treatment interventions to achieve improved outcomes, enhanced survival and quality of life for the cancer patient. The manuscript management system is completely online and includes a very quick and fair peer-review system, which is all easy to use. Visit http://www.dovepress.com/testimonials.php to read real quotes from published authors.

Submit your manuscript here: https://www.dovepress.com/cancer-management-and-research-journal